ISSN 1063-7729, Astronomy Reports, 2017, Vol. 61, No. 8, pp. 631–638. © Pleiades Publishing, Ltd., 2017.

Halo Density Profiles and Baryon Physics*

A. Del Popolo[1,2,3] ** **and Xi-Guo Li[♯1]**

[1] *Institute of Modern Physics, Chinese Academy of Sciences, Post Office Box 31, Lanzhou 730000, Peoples Republic of China*

[2] *Dipartimento di Fisica e Astronomia, Universitá di Catania, Viale Andrea Doria 6, 95125 Catania, Italy*

[3] *INFN, Sezione di Catania, Via Santa Sofia 64, 95123 Catania, Italy*

Received February 1, 2017; in final form, February 20, 2017

Abstract—The radial dependence of the pseudo phase-space density, $\rho(r)/\sigma^3(r)$ is studied. We find that the pseudo phase-space density for halos consisting both of dark matter and baryons is approximately a power-law only down to 0.1% of the virial radius while it has a non-power law behavior below the quoted scale, with inner profiles changing with mass. Halos consisting just of dark matter, as the one in dark matter only simulations, are characterized by an approximately power-law behavior. The results argue against universality of the pseudo phase-space density, when the baryons effect are included, and as a consequence argue against universality of density profiles constituted by dark matter and baryons as also discussed in [1].

DOI: 10.1134/S1063772917080029

1. INTRODUCTION

Despite the success of the Λ-CDM model that fits accurately the current observational data [2–6], the quoted model suffers from several problems, at small-scales (e.g., the cusp/core problem [7–10], the missing satellite problem, the too-big-to-fail problem [11–13], and on larger scales the cosmological constant problem [14, 15], and the cosmic coincidence problem.

An important issue in the Λ-CDM model is to determine the total mass of virialized halos [16–19] (galaxy and galaxy clusters) and their density profiles.

A decade ago it has been shown that the functional form of the universal profile of dark matter only haloes is well approximated by a profile whose logarithmic slope, $d\ln\rho/d\ln r \propto r^{\alpha}$, becomes increasingly shallower inwards (e.g., [20–22]). A unsolved question is whether the profile is actually universal or not [23–35].

In order to have more insights on the quoted problem, Taylor and Navarro [36] and Hansen [37] considered the radial run of the space density of N-body halos, $\rho(r)/\sigma^3(r)$.[1]

Taylor and Navarro [36] identified that the quantity $Q(r) = \rho/\sigma^3(r)$, which has become known as the pseudo phase-space density, behaves as a power law over 2–3 orders of magnitude in radius inside the virial radius. Other studies (e.g., [38, 39]) have confirmed the scale-free nature of $Q(r)$, and their results indicate that its slope lies in the range $\alpha = 1.90 \pm 0.05$. More recently, Ludlow et al. [40] calculated that the $Q(r)$ of Einasto halos should be close to power laws over a wide range of radii. However, very close to center for values of α typical of CDM halos $Q(r)$ deviates significantly from a power law.

Despite the insights obtained in previous studies [41–43], the origin for such universality of $Q(r)$ is not yet understood. The question of how this quantity relates to the true coarse-grained phase-space density has been investigated in several papers [43–47].

Moreover, some findings have called into question the universality of $\rho/\sigma(r)^3$. For instance, Schmidt et al. [48] have shown that simulated halos are better fit by a different power-law relation, and Ma et al. [49] found that $\rho/\sigma(r)^3$ is approximately a power law only over the limited range of halo radius resolvable by current simulations.

Moreover, all the previous quoted analysis do not study the possible effects produced by the presence of baryons on $\rho/\sigma(r)^3$, whose effect is to shallow [50–53] and to steepen [54–56] the dark matter profile. In collisionless N-body simulations, this complicated interplay between baryons and dark matter is not

*The text was submitted by the authors in English.

**E-mail: adelpopolo@oact.inaf.it

♯Corresponding author.

[1] $\sigma(r)$ is the one dimensional radial velocity dispersion.

taken into account, because it is very hard to include the effects of baryons in the simulations.

In the present paper, we focus on the study of the phase-space density proxy ρ/σ^3 in the case of dark matter and baryons halos, using the results of Del Popolo [1].

The paper is organized as follows. In Section 2 we summarize the Del Popolo [1] model. In Section 3 we discuss the results. Finally, Section 4 is devoted to conclusions.

2. SUMMARY OF THE METHOD

An often used model to study the non-linear evolution of perturbations of dark matter is the standard spherical collapse model (SSCM) introduced by Gunn and Gott [57] and extended in subsequent papers [58–72]. In the quoted model, a spherical density perturbation, divided into shells, evolves from the linear phase to the phase of maximum expansion (named turn-around), and then till the final collapse.

Knowing the initial comoving radius x_i, the mean fractional density excess inside the shell, $\overline{\delta}_i$, and the density parameter Ω_i, it is possible to obtain the final time averaged radius of a given Lagrangian shell [73]. If mass is conserved and each shell is kept at its turn-around radius, one can easily obtain the shape of the density profile [61, 73, 74] at turn-around. Starting from this, the final density profile is obtained assuming that the potential well near the center varies adiabatically [75, 76], which means that a shell near the center makes many oscillations before the potential changes significantly [75–77].

The model takes into account angular momentum, dynamical friction, and baryons adiabatic contraction. There are two sources of angular momentum of collisionless dark matter: (a) bulk streaming motions, and (b) random tangential motions. The first one (ordered angular momentum [58]) arises due to tidal torques experienced by proto-halos. The second one (random angular momentum [58]) is connected to random velocities (see [58]). Dynamical friction was calculated dividing the gravitational field into an average and a random component generated by the clumps constituting hierarchical universes. We took into account dynamical friction by introducing the dynamical friction force in the equation of motion (Eq. (A14) in [1]). The shape of the central density profile is influenced by baryonic collapse: baryons drag dark matter in the so called adiabatic contraction (AC), steepening the dark matter density slope. Blumenthal et al. [54] described an iterative approximate analytical model to calculate the effects of AC, solved with iterative techniques [78]. More recently Gnedin et al. [55] proposed a simple modification of the Blumenthal model, which describes numerical results more accurately. For systems in which angular momentum is exchanged between baryons and dark matter (e.g., through dynamical friction), Klypin et al. [56] introduced a modification to Blumenthal's model. The adiabatic contraction was taken into account by means of Gnedin et al. [55] model and Klypin et al. [56] model taking also account of exchange of angular momentum between baryons and dark matter.

In order to calculate $\rho(r)/\sigma^3(r)$, as Williams et al. [63], we determine for different halos their density profiles, $\rho(r)$ and $\sigma(r)$, using results of Del Popolo [1].

3. RESULTS AND DISCUSSIONS

A question that could be asked is the following: is the found power-law nature a real characteristic of all equilibrium N-body halos, at galactic scales or galaxy cluster scales, or has this kind of behavior been observed since $\rho(r)/\sigma^3(r)$ has been studied in a limited range of halo radius and without taking into account the effect of baryons? In order to answer this question and seeing if the same behavior is valid for halos of different masses, galaxies or clusters of galaxies, we shall use the SSCM model summarized in the previous section and fully described in [1] to calculate $\rho(r)/\sigma^3(r)$ in a wider radial range than that resolved by current simulations. Using [1], we generate two sets of halos with galaxy and cluster scale masses. Within each of the two sets, we study three different cases: in the case A we take into account all the effects included in [1], namely angular momentum, dynamical friction, baryons, adiabatic contraction of dark matter; in the case B there are no baryons and dynamical friction; in the case C only angular momentum is taken into account reduced in magnitude as in [1] in order to reproduce the angular momentum of N-body simulations (dashed line in [1, Fig. 2]) and a NFW profile (solid histogram in [1, Fig. 2]).

For what concerns the case C, we recall that in [1] we performed an experiment similar to that performed by Williams et al. [63] namely, we reduced the magnitude of the angular momentum by a factor of 2, and that of the dynamical friction force by a factor 2.5 with respect to the typical values calculated and used in the model in order to reproduce angular momentum of N-body simulations and the NFW profile.

3.1. Pseudo-Phase-Space Density: the Case of Galaxies and Clusters

In Fig. 1a we plot $\rho(r)/\sigma^3(r)$ with respect to radius, over 9 orders of magnitude, for a galaxy of 10^9 $M_\odot$. The solid, dotted and long-dashed lines

represent, respectively, the slope in the case A, the slope in the case B, and the slope in the case C. The short-dashed line represents the slope -1.9 found in several studies.[2] Figure 1b shows a zoom-in view of the portion of the left figure that is resolvable by current simulations: $0.003 \leq /r_{-2} \leq 30$.[3] Figure 1 illustrates that $\rho(r)/\sigma^3(r)$ is not a power-law in r both for cases A and B. In the cases A and B halos deviate strongly from a power-law at small radius. The zoom-in panels show, however, that the slope of $\rho(r)/\sigma^3(r)$ happens to be quite close to -1.9 over the limited range of $r/r_{-2} \simeq 0.001$ to 10 that is resolvable by current simulations. The deviations only start to show up at the smallest radius $r/r_{-2} \simeq 0.001$ near the simulation resolution limit. It is therefore not surprising that the power-law behavior of $\rho(r)/\sigma^3(r)$ continues to appear to be valid, even though the latest simulations find the Einasto form to be a better fit for $\rho(r)$ than GNFW (generalized NFW). If for ≥ 0.001 the $\rho(r)/\sigma^3(r)$ is more or less a power-law, the important point to note is that at radius smaller than $r/r_{-2} \leq 0.001$ $(10^{-7} \leq r/r_{-2} \leq 0.001)$, $\rho(r)/\sigma^3(r)$ deviates far away from a pure power law. For our cases A and B the shape of $\rho(r)/\sigma^3(r)$ flattens continuously towards the halo center. This is not unexpected since the corresponding density profile, as shown in [1], flattens toward the inner part of the halo, where it has a flat profile. As already reported, the density profile corresponding to the case C is characterized by the fact that we take into account only angular momentum reduced as in [1] in order to reproduce a NFW profile with inner slope $\rho \propto r^{-1}$. The corresponding $\rho(r)/\sigma^3(r)$ profile (long-dashed line in Fig. 1a) has an approximately power-law behavior with slope $\rho(r)/\sigma^3(r) \propto r^{-1.9}$ in agreement with several of the results in literature (e.g., [36]). It is worth noting, however, that even the NFW halo shows wiggles in the corresponding $\rho(r)/\sigma^3(r)$ profile; that is, NFW haloes have not an exact power-law $\rho(r)/\sigma^3(r)$.

At large radii, $r/r_{-2} \geq 1$, there is also a deviation of $\rho(r)/\sigma^3(r)$ from a power-law. The reason of this deviation can be explained by means of Jeans equation, as done in [63], and it is due to the fact that at large radii the equilibrium condition is not well satisfied. This apparently leads to a break in the scale-free behavior of $\rho(r)/\sigma^3(r)$ at large radii.

In Fig. 2 we plot $\rho(r)/\sigma^3(r)$ with respect to radius, in the case of a cluster of galaxies of 10^{14} $M_\odot$.

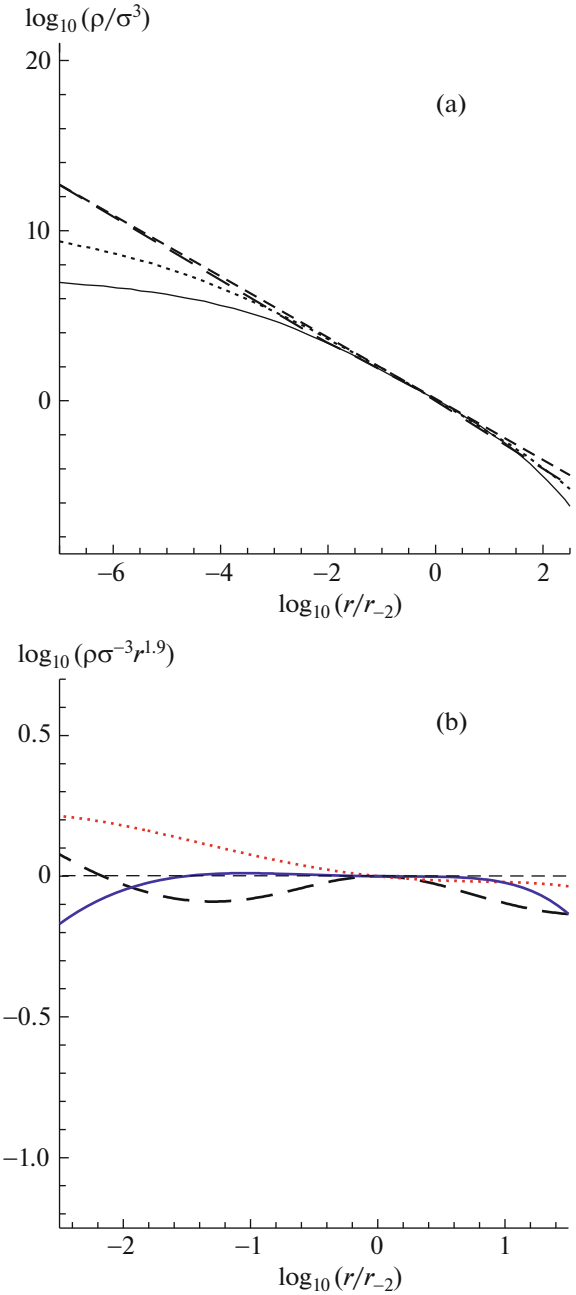

Fig. 1. Radial profiles of the pseudo-phase-space density for a 10^9 $M_\odot$ galaxy. (a) Solid line, dotted line, and long-dashed line represent, respectively, the pseudo-phase-space density for the cases A, B, and C described in the paper. The short-dashed line represents the slope -1.9 found in several studies (see the Introduction). (b) Show a zoom-in view of the portion of the left figure, multiplied by $r^{1.875}$, that is resolvable by current simulations. Symbols are as in (a).

Here, the solid line, the dotted line, and the dashed line represents case A, case B, and case C. The behavior of the phase-space proxy is similar to the case of the galaxy. Also in this case at small and large radii $\rho(r)/\sigma^3(r)$ is not a power-law, but in a different radius range with respect to galaxies, namely

[2] As reported in the introduction some studies, e.g., Ascasibar et al. [39], showed that the slope $\alpha = 1.90 \pm 0.05$, compatible with Taylor and Navarro [36] value of $\alpha = -1.875$.

[3] r_{-2} is the radius at which the logarithmic slope of the space density is -2.

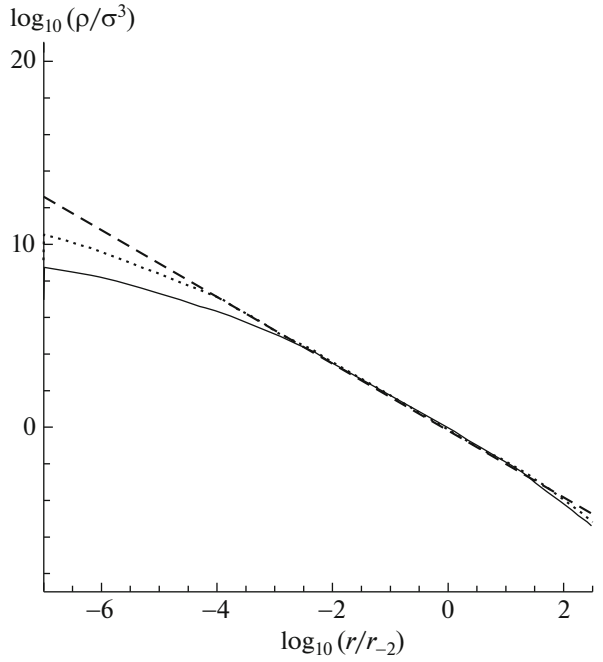

Fig. 2. Radial profiles of the pseudo-phase-space density for a 10^{14} $M_\odot$ cluster. Solid line, dotted line, and long-dashed line represent, respectively, the pseudo-phase-space density for the cases A, B, and C described in the paper.

$10^{-7} \leq r/r_{-2} \leq 0.01$ and $r/r_{-2} \leq 10$. Moreover, the $\rho(r)/\sigma^3(r)$ slope of both cases A and B, for small radii, are steeper than in the case of the galaxy, and the slope of curve relative to the NFW profile (dashed line) is slightly less steep, namely $\rho/\sigma^3 \propto r^{-0.8}$, in agreement with Williams et al. [63] results.

In order to explain why the inner $\rho(r)/\sigma^3(r)$ profiles are not power-laws and why the slopes are steeper in the cluster of galaxies case, we have to recall how the density profiles, $\rho(r)$, are formed in [1]. The differences in slopes with mass for the three plotted cases (A, B, and C) can be explained as follows. In case A, baryons, dynamical friction and angular momentum are present. The final density profile and final slope are determined by the interplay of these three factors.

The quoted effects act in a complicated interplay. Initially, at high redshift (e.g., $z = 50$), the density profile is in the linear regime. The profile evolves to the non-linear regime, and virializes. At an early redshift, (e.g., $z \simeq 5$ for dwarf galaxies), the dark matter density experiences the adiabatic contraction by baryons producing a slightly more cuspy profile. The evolution after virialization is produced by secondary infall, two-body relaxation, dynamical friction and angular momentum. Angular momentum contributes to reduce the inner slope of density profiles by preventing particles from reaching halo's center, while dynamical friction dissipates the clumps orbital energy and deposits it in the dark matter with the final effect of erasing the cusp (similarly to [50–52, 79]. The cusp is slowly eliminated and within $\simeq$1 kpc a core forms for objects of the mass of dwarf-galaxies. It is now clear why going from a model which takes into account baryons, dynamical friction, and angular momentum (solid line, case A) to the one taking into account just the angular momentum (dashed line, case B) and to the one taking into account just the angular momentum reduced to reobtain N-body simulations angular momentum, one obtains so different behavior of inner density profile slopes.

The main reason of the difference of behavior between clusters and galaxies is due to the fact that in the case of clusters the virialization process starts much later with respect to galaxies. In the case of galaxies, the profile strongly evolves after virialization through the processes previously described. In the case of dwarf galaxies of 10^9 $M_\odot$, we showed in [1] that the profile virializes at $z \simeq 10$ and from this redshift to $z = 0$ its shape continues to evolve, except at $z \simeq 5$ when adiabatic contraction steepens the profile. In the case of a cluster of 10^{14} $M_\odot$, the profile virializes at $z \simeq 0$ [1] and, as a consequence, the further evolution observed in galaxies cannot be observed in clusters. Summarizing, Figs. 1 and 2 show that $\rho(r)/\sigma^3(r)$ is not a power-law as shown in some previous studies mentioned in the introduction. Our results are in line with some recent work that has called into question the universality of $\rho/\sigma(r)^3$. For instance, Schmidt et al. [48] have advocated that individual simulated haloes are better fitted by a generalized power-law relation that is not necessarily $\rho/\sigma(r)^3$:

$$\frac{\rho}{\sigma_D^\epsilon} \propto r^{-\alpha}, \qquad (1)$$

where $\sigma_D = \sigma_r\sqrt{1 + D\beta}$, and D parameterizes a generalized σ_D; for instance, $D = 0$ and -1 correspond to $\sigma_D = \sigma(r)$, and σ_t, respectively.[4] Schmidt et al. [48] showed that the best-fit values of (D, ϵ, α) differ from halo to halo, and as a set, they roughly follow the linear relations $\epsilon = 0.97D + 3.15$ and $\alpha = 0.19D + 1.94$. For $\sigma = \sigma(r)$ (i.e., $D = 0$), the optimal relation is $\rho/\sigma(r)^{3.15} \propto r^{-1.94}$, which is consistent with the reported behavior of $\rho/\sigma(r)^3$ in N-body simulations within error bars. Similarly, Ma et al. [49], examining the radial dependence of $\rho/\sigma(r)^3$ over 12 orders of magnitude in radius by solving

[4] Note that $\sigma(r)$, and σ_t, are the one dimensional radial and tangential velocity dispersions, and are the same used by Schmidt et al. [48] through simulations.

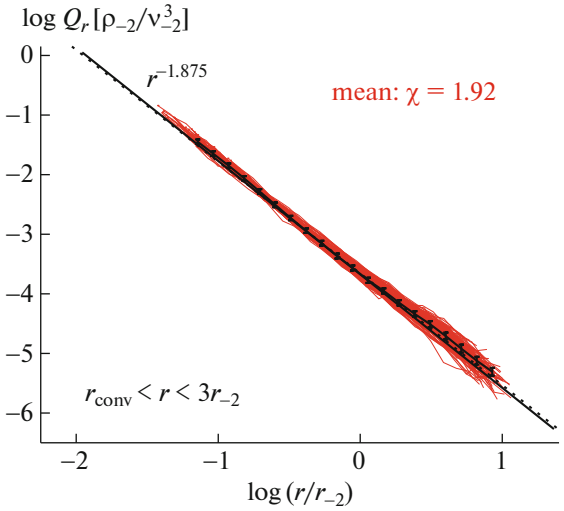

Fig. 3. Comparison of pseudo-phase-space density profiles in [40, Fig. 2], with the result of the present paper (solid line).

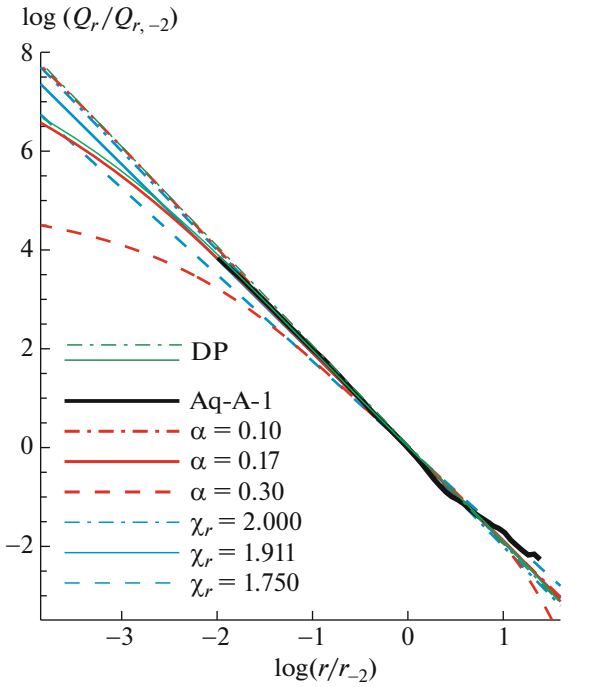

Fig. 4. Comparison of pseudo-phase-space density profiles in [40, Fig. 5b] with those obtained in the present paper. The result of the present paper (solid green line) for case B is in good agreement with pseudo-phase-space density profile of Einasto profile with $\alpha = 0.17$ typical of Λ-CDM models and the case $\alpha = 0.10$ is almost identical to that of the present paper for case C (green dashed line). DP stands for Del Popolo (i.e., the result of the present paper).

the Jeans equation for a broad range of input ρ and velocity anisotropy β, found that $\rho/\sigma(r)^3$ is approximately a power law only over the limited range of halo radius resolvable by current simulations (down to $\sim$0.1% of the virial radius), and $\rho/\sigma(r)^3$ deviates significantly from a power-law below this scale for both the Einasto and NFW density profiles, $\rho(r)$.

3.2. Simulations Versus Our DM Density Profiles and $\rho(r)/\sigma^3(r)$

In order to show how our results concerning $\rho(r)/\sigma^3(r)$ are in agreement with high-resolution simulations, in the radius range that they studied, we compare the results for $\rho(r)/\sigma^3(r)$ with recent results of Ludlow et al. [40], who calculated the pseudo phase-space density for the Einasto profile.

In Fig. 3 of the present paper we show the top panel of Fig. 2 of Ludlow et al. [40]. In Fig. 3, the mean profiles and one-sigma scatter of Q calculated in [40] are shown as solid red lines with error bars. The dotted curve shows Bertschinger $r^{-1.875}$ result, while the solid black line, almost indistinguishable from the dotted line, was calculated with the model of the present paper without taking into account baryons, in order to be able to compare the result with dissipationless simulations results for Q, like those of [40]. Fig. 3 shows a very good agreement of the result of the present paper with those of [40], in their studied radius range $\simeq 10^{-2}$–$10^{1.5}$.

Note that χ in Fig. 3 is the exponent in

$$Q(r) = \frac{\rho}{\sigma^3} = \frac{\rho_o}{\sigma_o^3}\left(\frac{r}{r_o}\right)^{-\chi}, \qquad (2)$$

which as previously told was originally reported in [36].

Figure 4 shows (in blue) the density profiles for three different values of χ and compares them to Einasto profiles. The values of α of the three Einasto profiles shown have been chosen by [40] to match as closely as possible the profiles corresponding to the pseudo phase-space density models. Figure 4 shows (in red) the pseudo phase-space density profiles of Einasto halos for three different values of α. For $\alpha = 0.1$ and 0.17 the corresponding pseudo phase-space density profiles are very well approximated by power laws over the whole plotted radial range.

Only for larger values of α such as 0.3, clear deviations from a power law are noticeable. The thick solid black curve shows the profile corresponding to the billion-particle Aq-A-1 halo, namely Navarro et. [22] highest resolution halo. The solid (dot-dashed) green line marked DP in Fig. 4 plots the pseudo phase-space density profile calculated with the model of the present paper for case B (C). The green dashed line in Fig. 4 shows that the flattening that we obtain at $r/r_{-2} = 10^{-3.7}$ (smallest value plotted in [40,

Fig. 5b]) is close to the case $\alpha = 0.17$ (typical of Λ-CDM models), plotted in [40, Fig. 5b]. The flattening in [40, Fig. 5b] for $\alpha = 0.10$ at $r/r_{-2} = 10^{-3.7}$ is almost identical to that of the present paper for case C (green dot-dashed line).

Figure 4 shows a very good agreement of the result of the present paper with those in [40], in their studied radius range $\simeq 10^{-3.7}-10^{1.5}$ both for an Einasto profile with $\alpha = 0.17$ and 0.10. Ludlow et al. [40] did not probe pseudo-phase-space density profile at a smaller radius, as done in the present paper. At a radius of $\simeq 10^{-3.7}$, minimum radius plotted by Ludlow et al. [40], a small discrepancy from pure power-law behavior of the pseudo-phase-space density profile starts to be seen, and if one goes to a smaller radius (e.g., 10^{-9} as in the submitted paper) the flattening should be larger. Moreover, as reported in the Conclusion section in [40]: "significant differences are only expected at radii well inside 1% of the scale radius, r_{-2}, and are therefore beyond the reach of current simulations."

3.3. Halo Density Profiles and the Phase-Space Density Profile

Another issue to discuss is the interrelation between the universality of the pseudo-phase-space density and that of the halos density profiles. As previously discussed, there are different methods to analyze dark matter halos structure. A standard approach involves investigating the halos density profiles. Few theoretical attempts have been made to understand the origin of this density profile (e.g., [80, 81]), with varying level of success. The scale-free nature of $\rho(r)/\sigma^3(r)$ represents a novel way of looking at the properties of halos. If this property is "universal", it amounts to a hitherto unrecognized constraint on the shape of the density profiles [41]. Our result confirm this point of view: $\rho(r)/\sigma^3(r)$ profiles flattening toward the halo center is generated by similar density profiles, which have logarithmic slope $\alpha \simeq 0$ for 10^8-10^9 $M_\odot$ and $\alpha \simeq 0.6$ for $M \simeq 10^{14}$ $M_\odot$ [1].

At the same time, our main result is that $\rho(r)/\sigma^3(r)$ is not universal if studied in the appropriate radius range, and similarly we expect that halos density profiles are not universal, because their inner part should depend on mass, as the $\rho(r)/\sigma^3(r)$ profiles, and should also flatten toward the halo center, showing flat cores in the center of the halo (as shown in [1]). This result is in agreement with several previous ones, described in the reminder.

Ricotti's [26] N-body simulations suggested that the density profile of DM haloes is not universal (in agreement with the other cited studies), but that there are instead shallower cores in dwarf galaxies and steeper cores in clusters. This leads to the conclusion that density profiles do not have a universal shape (see also [24, 29–31, 82].

There are also observational evidences of a mass dependence of the dark matter density profile. Simon [83–85] removed the contribution of the stellar disk to the rotation curve of 5 galaxies in order to reveal the rotation curve of their dark matter halo. They found that the galaxies NGC 2976, NGC 6689, NGC 5949, NGC 4605, NGC 5963 have very different values of the slope: $\alpha \simeq 0.01$, 0.80, 0.88, 0.88, 1.28, respectively. By using the THINGS sample, de Blok et al. [86] concluded that galaxies brighter than $M_B > -19$ have profiles that can be equally well described by cored or cuspy profiles, while those with $M_B < -19$ are best fitted by cuspy profiles.

In the case of clusters, Host and Hansen [87] took a sample of 11 highly relaxed clusters and used the measurements of the X-ray emitting gas to infer model-independent mass profiles. They then made comparisons with a number of different models that have been applied as mass profiles in the literature, concluding that there is a strong indication that this inner slope needs to be determined for each cluster individually. This implies that X-ray observations do not support the idea of a universal inner slope, but perhaps hint at a dependence with redshift or mass. Similar result comes from the studies of Sand et al. [88–92], which studied the external parts of several clusters through weak lensing, and the inner one through strong-lensing and stellar dynamics.

Before concluding, I would like to mention that the equations in the present paper have similarities to those in the study of Sapar [93], in which non-relativistic low-velocity massive neutrinos (or a generic weak-interacting particle) have cooled down to very low temperatures and velocities, so that they may affect the evolution of halos. Interestingly, in that scenario cores are formed in the galactic center, instead of the cusps predicted by simulation.

4. CONCLUSIONS

In the present paper, we checked if the pseudo phase-space density, $\rho(r)/\sigma^3(r)$, behaves as a power law over 2–3 orders of magnitude in radius inside the virial radius by means of the model described in [1]. We find that $\rho(r)/\sigma^3(r)$ is not in general a power-law for the case A (dark matter and baryons) and B (no baryons) described in the paper. In the radial range probed by current N-body simulations (down to 10^{-3} virial radii), $\rho(r)/\sigma^3(r)$ approximately behaves like a power-law, while for radial scales below the resolution of current simulations, there are significant deviations

from a power-law profile. A similar, non-power-law behavior is observed at large radii (>10 virial radii). In the paper, we also set the angular momentum and dynamical friction so that the density profile is approximately a NFW profile (case C). In this case $\rho(r)/\sigma^3(r)$ is approximately a power law. The pseudo phase-space density was calculated for structures on galactic, and cluster of galaxy mass scale. The behavior of $\rho(r)/\sigma^3(r)$ observed was similar, but in the case of clusters the slope was steeper in both cases A and B. This difference is connected to the different redshift at which the two class of objects formed, larger for galaxies, smaller for clusters, which implies a longer time at disposal of galaxies to evolve. The results of the quoted study are in agreement with those of Schmidt et al. [48] and Ma et al. [49]. We conclude that radial profiles of the pseudo phase-space density corresponding to density profiles which flatten going towards the halo center cannot be power laws, and the prediction of N-body simulations of a power-law behavior in $\rho(r)/\sigma^3(r)$ is due just to the fact that the pseudo phase-space density is observed only down to a resolution limit of 10^{-3} virial radii.

The results argue against universality of the pseudo phase-space density and as a consequence argue against universality of density profiles constituted by dark matter and baryons as also discussed in [1].

ACKNOWLEDGMENTS

The present work was supported by the Chinese Academy of Sciences and by the President's international fellowship initiative, grant no. 2017 VMA0044.

REFERENCES

1. A. Del Popolo, Astrophys. J. **698**, 2093 (2009).
2. E. Komatsu, K. M. Smith, Dunkley J., C. L. Bennett, et al., Astrophys. J. Suppl. **192**, 18 (2011).
3. S. W. Allen, A. E. Evrard, and A. B. Mantz, Ann. Rev. Astron. Astrophys. **49**, 409 (2011).
4. A. Del Popolo, Astronomy Reports **51**, 169 (2007).
5. A. Del Popolo, IX Mexican School on Gravitation and Mathematical Physics: Cosmology for the XXIst Century: Gravitation and Mathematical Physics Division of the Mexican Physical Society (DGFM-SMF), AIP Conf. Proc. **1548**, 2 (2013).
6. A. Del Popolo, International J. Modern Physics D **23**, id. 1430005 (2014).
7. V. F. Cardone and A. Del Popolo, Monthly Not. Roy. Astron. Soc. **427**, 3176 (2012).
8. A. Del Popolo, V. F. Cardone, and G. Belvedere, Monthly Not. Roy. Astron. Soc. **429**, 1080 (2013).
9. A. Saburova and A. Del Popolo, Monthly Not. Roy. Astron. Soc. **445**, 3512 (2014).
10. A. Del Popolo and N. Hiotelis, J. Cosmology and Astroparticle Phys. **01**, id. 047 (2014).
11. A. Del Popolo and M. Gambera, Astron. and Astrophys. **321**, 691 (1997).
12. A. Del Popolo, J. A. S. Lima, J. C. Fabris, and D. C. Rodrigues, J. Cosmology and Astroparticle Phys. **04**, id. 021 (2014).
13. A. Del Popolo and M. Le Delliou, J. Cosmology and Astroparticle Phys. **12**, id. 051 (2014).
14. S. Weinberg, Rev. Modern Physics **61**, 1 (1989).
15. A. V. Astashenok and A. Del Popolo, Class. Quant. Grav. **29** (2012).
16. A. Del Popolo and M. Gambera, Astron. and Astrophys. **308**, 373 (1996).
17. A. Del Popolo, Monthly Not. Roy. Astron. Soc. **336**, 81 (2002).
18. N. Hiotelis and A. Del Popolo, Astrophys. Space Sci. **301**, 67 (2006).
19. N. Hiotelis and A. Del Popolo, Monthly Not. Roy. Astron. Soc. **436**, 163 (2013).
20. J. F. Navarro, E. Hayashi, C. Power, A. R. Jenkins, C. S. Frenk, S. D. M. White, V. Springel, J. Stadel, and T. R. Quinn, Monthly Not. Roy. Astron. Soc. **349**, 1039 (2004).
21. J. Stadel, D. Potter, B. Moore, J. Diemand, P. Madau, M. Zemp, M. Kuhlen, and V. Quilis, Monthly Not. Roy. Astron. Soc. **398**, 21 (2009).
22. J. F. Navarro, A. Ludlow, V. Springel, J. Wang, et al., Monthly Not. Roy. Astron. Soc. **402**, 21 (2010).
23. B. Moore, F. Governato, T. Quinn, J. Stadel, and G. Lake, Astrophys. J. **499**, L5 (1998).
24. K. Subramanian, R. Cen, and J. P. Ostriker, Astrophys. J. **538**, 528 (2000).
25. A. Klypin, A. V. Kravtsov, J. S. Bullock, and J. R. Primack, Astrophys. J. **554**, 903 (2001).
26. M. Ricotti, Monthly Not. Roy. Astron. Soc. **344**, 1237 (2003).
27. M. Ricotti, A. Pontzen, and M. Viel, Astrophys. J. **663**, 53 (2007).
28. T. Fukushige, A. Kawai, and J. Makino, Astrophys. J. **606**, 625 (2004).
29. R. Y. Cen, F. Dong, P. Bode, and J. P. Ostriker, arXiv: astro-ph/0403352v2 (2004).
30. D. Merritt, A. W. Graham, B. Moore, J. Diemand, and B. Terzic, Astron. J. **132**, 2685 (2006).
31. A. W. Graham, D. Merritt, B. Moore, J. Diemand, B. Terzic, Astron. J. **132**, 2701 (2006).
32. L. Gao, J. F. Navarro, S. Cole, C. S. Frenk, et al., Monthly Not. Roy. Astron. Soc. **387**, 536 (2008).
33. A. Del Popolo, Monthly Not. Roy. Astron. Soc. **408**, 1808 (2010).
34. Yu. V. Babyk, A. Del Popolo, and I. B. Vavilova, Astron. Rep. **58**, 587 (2014).
35. A. Del Popolo, J. Cosmology and Astroparticle Phys. **07**, id. 019 (2014).
36. J. E. Taylor and J. F. Navarro, Astrophys. J. **563**, 483 (2001).
37. S. H. Hansen, Monthly Not. Roy. Astron. Soc. **352**, L41 (2004).
38. E. Rasia, G. Tormen, and L. Moscardini, Monthly Not. Roy. Astron. Soc. **351**, 237 (2004).
39. Y. Ascasibar, G. Yepes, and S. Gottlober, Monthly Not. Roy. Astron. Soc. **352**, 1109A (2004).

40. A. D. Ludlow, J. F. Navarro, S. D. M. White, M. Boylan-Kolchin, V. Springel, A. Jenkins, and C. S. Frenk, Monthly Not. Roy. Astron. Soc. **415**, 3895 (2011).
41. C. G. Austin, L. L. R. Williams, E. I. Barnes, A. Babul, and J. J. Dalcaton, Astrophys. J. **634**, 756 (2005).
42. E. I. Barnes, L. L. R. Williams, A. Babul, and J. J. Dalcanton, Astrophys. J. **643**, 797 (2006).
43. Y. Hoffman, E. Romano-Diaz, I. Shlosman, and C. Heller, Astrophys. J. **671**, 1108 (2007).
44. I. M. Vass, S. Kazantzidis, M. Valluri, and A. V. Kravtsov, Astrophys. J. **698** (2), 1813 (2009).
45. I. M. Vass, M. Valluri, A. V. Kravtsov, and S. Katzandis, Monthly Not. Roy. Astron. Soc. **395** (3), 1225 (2009).
46. M. Maciejewski, S. Colombi, C. Alard, F. Bouchet, and C. Pichon, Monthly Not. Roy. Astron. Soc. **393**, 703 (2009).
47. S. Sharma and M. Steinmetz, Monthly Not. Roy. Astron. Soc. **373**, 1293 (2006).
48. K. B. Schmidt, S. H. Hansen, and A. V. Maccio, Astrophys. J. **689**, L33 (2008).
49. C.-P. Ma, P. Chang, and J. Zhang, arXiv: 0907.3144 [astro-ph.CO] (2009).
50. A. El-Zant, I. Shlosman, and Y. Hoffman, Astrophys. J. **560**, 636 (2001).
51. A. El-Zant, Y. Hoffman, J. Primack, F. Combes, and I. Shlosman, Astrophys. J. **607**, 75 (2004).
52. E. Romano-Diaz, I. Shlosman, Y. Hoffman, and C. Heller, Astrophys. J. **685**, L105 (2008).
53. E. Romano-Diaz, I. Shlosman, C. Heller, and Y. Hoffman, Astrophys. J. **702**, 1250 (2009).
54. G. R. Blumenthal, S. M. Faber, R. Flores, and J. R. Primack, Astrophys. J. **301**, 27 (1986).
55. O. Y. Gnedin, A. V. Kravtsov, A. A. Klypin, and D. Nagai, Astrophys. J. **616**, 16 (2004).
56. A. Klypin, H. Zhao, and R. S. Somerville, Astrophys. J. **573**, 597 (2002).
57. J. E. Gunn and J. R. Gott, Astrophys. J. **176**, 1 (1972).
58. B. S. Ryden and J. E. Gunn, Astrophys. J. **318**, 15 (1987).
59. A. V. Gurevich and K. P. Zybin, Zh. Eksp. Teor. Fiz. **94**, 3 (1998).
60. A. V. Gurevich and K. P. Zybin, Zh. Eksp. Teor. Fiz. **94**, 5 (1998).
61. S. D. M. White and D. Zaritsky, Astrophys. J. **394**, 1 (1992).
62. P. Sikivie, I. I. Tkachev, and Y. Wang, Physical Review D **56**, 1863 (1997).
63. L. L. R. Williams, A. Babul, and J. J. Dalcanton, Astrophys. J. **604**, 18 (2004).
64. A. Del Popolo and P. Kroupa, Astron. and Astrophys. **502**, 733 (2009).
65. V. F. Cardone, A. Del Popolo, C. Tortora, and N. R. Napolitano, Monthly Not. Roy. Astron. Soc. **416**, 1822 (2011).
66. V. F. Cardone, M. P. Leubner, and A. Del Popolo, Monthly Not. Roy. Astron. Soc. **414**, 2265 (2011).
67. A. Del Popolo, Monthly Not. Roy. Astron. Soc. **419**, 971 (2012).
68. A. Del Popolo, Monthly Not. Roy. Astron. Soc. **424**, 38 (2012).
69. A. Del Popolo, F. Pace, and J. A. S. Lima, Monthly Not. Roy. Astron. Soc. **430**, 628 (2013b).
70. A. Del Popolo, F. Pace, and J. A. S. Lima, International J. Modern Physics D **22**, id. 1350038 (2013).
71. A. Del Popolo, F. Pace, S. P. Maydanyuk, J. A. S. Lima, and J. F. Jesus, Physical Review D **87**, id. 043527 (2013).
72. F. Pace, R. C. Batista, and A. Del Popolo, Monthly Not. Roy. Astron. Soc. **445**, 648 (2014).
73. P. J. E. Peebles, *The Large Scale Structure of the Universe* (Princeton, Princeton Univ. Press, 1980).
74. Y. Hoffman and J. Shaham, Astrophys. J. **297**, 16 (1985).
75. J. E. Gunn, Astrophys. J. **218**, 592 (1977).
76. J. A. Filmore and P. Goldreich, Astrophys. J. **281**, 1 (1984).
77. S. Zaroubi and Y. Hoffman, Astrophys. J. **416**, 410 (1993).
78. E. Spedicato, E. Bodon, A. Del Popolo, and N. Mahdavi-Amiri, Quarterly J. Operations Research **1** (1), 51 (2003).
79. C. Tonini, A. Lapi, and P. Salucci, Astrophys. J. **649**, 591 (2006).
80. E. Salvador-Sole, A. Manrique, G. Gonza'lez-Casado, and S. H. Hansen, Astrophys. J. **666**, 181 (2007).
81. R. N. Henriksen, Astrophys. J. **671**, 1147 (2007).
82. D. Merrit, J. F. Navarro, A. Ludlow, and A. Jenkins, Astrophys. J. **624**, L85 (2005).
83. J. D. Simon, A. D. Bolatto, A. Leroy, and L. Blitz, Astrophys. J. **596**, 957 (2003).
84. J. D. Simon, A. D. Bolatto, A. Leroy, and L. Blitz, in *Satellites and Tidal Streams*, Ed. by F. Prada, D. Martinez Delgado, and T. J. Mahoney, Astron. Soc. Pacific **327**, 18 (2003) (2004).
85. J. D. Simon, A. D. Bolatto, A. Leroy, L. Blitz, and E. L. Gates, Astrophys. J. **621**, 757 (2004).
86. W. J. G. de Blok, F. Walter, E. Brinks, C. Trachternach, S.-H. Oh, and Jr. R. C. Kennicutt, Astron. J. **136**, 2648 (2008).
87. O. Host and S. H. Hansen, astro-ph/0907.1097v1 (2009).
88. D. J. Sand, T. Treu, and R. S. Ellis, Astrophys. J. **574**, L129 (2002).
89. D. J. Sand, T. Treu, G. P. Smith, and R. S. Ellis, Astrophys. J. **604**, 88 (2004).
90. D. J. Sand, T. Treu, R. S. Ellis, G. P. Smith, and J. P. Kneib, Astrophys. J. **674**, 711 (2008).
91. A. B. Newman, T. Treu, R. S. Ellis, and D. J. Sand, Astrophys. J. **765**, 25 (2013).
92. A. B. Newman, T. Treu, R. S. Ellis, D. J. Sand, C. Nipoti, J. Richard, and E. Jullo, Astrophys. J. **765**, 24 (2013).
93. A. Sapar, Baltic Astronomy **23**, 71 (2014).